AQUA
Water Infrastructure, Ecosystems and Society

IWA PUBLISHING

 AQUA — Water Infrastructure, Ecosystems and Society Vol 72 No 10, 1867 doi: 10.2166/aqua.2023.105

Thermodynamic performance assessment of a community-scale brackish water reverse osmosis plant using exergy analysis

Bhaumik Sutariya [a,b,*] and Govind Amaliar[a]

[a] Membrane Science and Separation Technology Division, CSIR-Central Salt and Marine Chemicals Research Institute, G.B. Marg, Bhavnagar, Gujarat 364002, India
[b] Academy of Scientific and Innovative Research (AcSIR), Ghaziabad 201002, India
*Corresponding author. E-mail: bhaumiks@csmcri.res.in

BS, 0000-0002-1247-2043

ABSTRACT

This study investigated the thermodynamic performance of a community-scale membrane-based brackish water reverse osmosis (BWRO) plant at various operating pressures from 13.79 to 27.58 bar and feed salinity levels from 2,000 to 20,000 mg/L. We aimed to identify the components responsible for the exergy losses and to suggest improvements. The results showed that the exergetic efficiency of some individual components had a significant impact on the performance of the desalination plant, where the high-pressure (HP) pump assembly and pressure control valve were identified as the major contributors to exergy losses (57.83–70.59 and 15.75–27.62%, respectively). The inefficiency of the feed pump assembly contributed to 11–12% of the total destruction of exergy under different operating conditions. The analysis further revealed that the exergetic efficiency of the plant was maximum (0.51%) at the feed salinity of 10,000 mg/L and operating pressure of 27.58 bar. It was minimum (0.01%) for the highest salinity (20,000 mg/L) and the lowest operating pressure (13.79 bar), due to the low requirement of work of separation and higher fixed losses. The exergetic efficiency was also correlated to the energetic performance of the BWRO plant at different operating conditions.

Key words: desalination, efficiency, exergy, reverse osmosis

HIGHLIGHTS

- A decentralized community-scale BWRO plant was analyzed using exergy analysis.
- The exergetic efficiency of the RO system was very low (i.e. 0.01–0.51%).
- The major contributors to the exergy destruction were identified as the pump assemblies and the pressure control valve.
- The effects of operating conditions on the ergetic efficiency was also studied and ways to improve the efficiency were discussed.

GRAPHICAL ABSTRACT

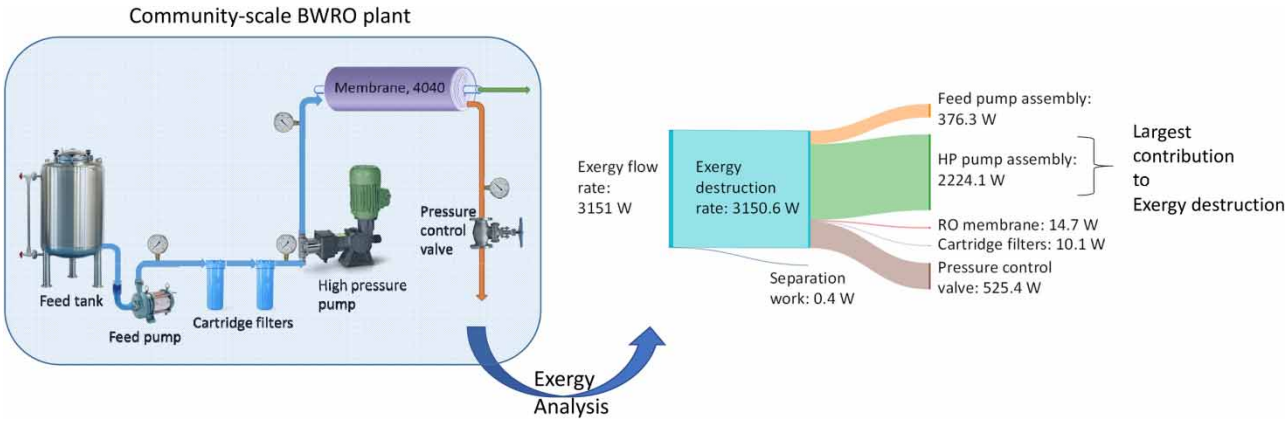

1. INTRODUCTION

In recent years, there has been a growing need for sustainable and efficient water treatment technologies to address the increasing demand for freshwater in many parts of the world (Boretti & Rosa 2019). Reverse osmosis (RO) is a popular water treatment technology that uses a semi-permeable membrane to remove dissolved salts and other contaminants from seawater, brackish water, and wastewater. However, the energy-intensive nature of the RO processes and their impact on the environment has led to increased interest in optimizing their performance through exergy analysis.

Exergy analysis is a thermodynamic approach that evaluates the quality of energy and its ability to perform useful work in a system. It provides a comprehensive framework for assessing the efficiency of energy conversion processes, identifying sources of energy losses, and optimizing the performance of the system. In the context of the RO processes, exergy analysis can help identify the sources of energy losses, such as membrane characteristics, pump inefficiencies, and pressure drops across components, and propose measures to reduce them. Although the energy flow analysis also does the same, exergy analysis is preferred as it captures the quality of separation along with the efficiency. For example, even if the energetic efficiency of the system to generate an equal amount of product water of two different salinity levels are equal, their exergetic efficiency will be different due to the different quality of the product and the reject. The insights gained from exergetic efficiency analysis along with techno-economic analysis guide decision-making, allowing for the implementation of targeted measures to reduce energy waste and maximize the utilization of high-quality energy. Ultimately, this comprehensive approach leads to improved energy efficiency, reduced environmental impact, and increased economic viability of RO systems.

Numerous studies have conducted exergy analyses on membrane-based RO plants, which have identified the sites where irreversibilities occur. For instance, Kahraman *et al.* (2005) investigated a desalination plant in California that utilized two-stage RO, nanofiltration (NF), and electrodialysis reversal (EDR) with brackish water feed and no energy recovery device (ERD) and found that the RO modules and pumps caused the most exergy destruction. The RO unit in the plant had an exergetic efficiency of 8.0%, the NF unit had a 9.7% efficiency, and the EDR unit had an efficiency of 6.3%. In another study, Ajundi (2009) examined a two-stage RO desalination plant with brackish water feed and no ERD and discovered that the exergetic efficiency was only 4.1%. The main sources of irreversibility were the four throttle valves and the RO modules. It is important to note that the exergetic efficiencies vary due to factors such as feed water salinity, flow rate, pump efficiency, energy recovery device choice, the definition of exergetic efficiency, and exergy destruction in the throttle valves.

Exergy study has been utilized to study the best-suited type of energy recovery device (ERD). For example, Eshoul *et al.* (2017); Nuri *et al.* (2017) studied a proposed 24,000 m^3/day RO plant in Libya to improve efficiency and reduce power consumption. The study focused on the effect of PX (pressure exchanger) and ERT (energy recovery turbine) modifications on the performance of four different seawater RO configurations. They found that combining PX and ERT resulted in the optimal configuration, with the highest exergy efficiency, lowest membrane area, lowest specific power consumption, and product cost. This combination allowed for energy recovery at both stages, leading to significant cost savings over the lifetime of the desalination plant. Bouzayani *et al.* (2009) modeled three systems, which included PX and ERT, that combine RO with a steam power plant to produce drinkable water. Depending on the nature of the ERD in the RO subsystem and the presence of thermal coupling between the two subsystems, three cases are analyzed, and the quantity and quality of drinkable water produced, along with energy and exergy efficiencies, were compared for identical operating conditions. The analysis showed that the systems with a PX and thermal coupling produce the highest amount of drinkable water and the highest power available for electricity generation.

Cerci (2002), Kahraman & Cengel (2005), Aljundi (2009), and others have defined exergetic efficiency by comparing the exergy of both permeate and reject outflow to the exergy input by the pumps. However, it was argued by Ahmed & Syed (2016) that the exergy output should only be based only on the permeate outlet, it being the useful stream. Nonetheless, sometimes the reject stream can be utilized for other purposes, such as salt production (Mushtaque *et al.* 2003) or further treatment (Ahmed 2017; Im *et al.* 2021; Tra *et al.* 2022). Therefore, the calculation of exergetic efficiency based on both the exergies of permeate and reject outflow is more appropriate.

The majority of exergy analysis studies for membrane-based desalination processes have been conducted on large-scale seawater RO) plants (Eshoul *et al.* 2015, 2017) or brackish water RO (BWRO) plants (Romero-Ternero *et al.* 2005; Eshoul *et al.* 2016; Fellaou *et al.* 2021; Alsarayreh *et al.* 2022). However, there is a gap in the literature regarding the exergy analysis of decentralized community-scale BWRO plants, which are prevalent in remote rural and coastal areas (Joshi *et al.* 2004;

Anas *et al.* 2021; Que *et al.* 2021). As the energy consumption of these plants continues to rise, it has become crucial to investigate the exergetic efficiency of their components in order to identify areas of irreversibility and improve their sustainability.

In this study, we conducted an exergy analysis of a community-scale membrane-based BWRO plant, with an emphasis on the performance of our lab-made membrane, efficiency of the pump assemblies, and performance of the pressure control valve. Being a community-scale BWRO plant, we did not consider the use of an energy recovery device. We aimed to evaluate exergetic efficiency of the plant, identify sources of energy losses, and propose measures to improve its performance.

2. METHODOLOGY

2.1. Plant description

The setup consisted of a 150-L feed storage tank that was connected to a feed water pump manufactured by Grundfos India with the model number CRN1S-8 A-P-G-V-HQQV. The discharge of this pump was then connected to two polypropylene spun cartridge filters, each of which was 10 inches long and manufactured by Gopani Product Systems India. A positive displacement high-pressure (HP) pump with the model HV-22, manufactured by ASPEE India, was connected to a two horsepower induction motor (Crompton Greaves India) via two v-belts (JK Fenner Poly-F Plus A1000/A38). The diameters of the pulleys connected to the motor and the pump were 3 and 8 inches (7.6 and 20.32) cm. The discharge of the HP pump was then connected to a pressure vessel that was manufactured by Pentair India and had the model number Codeline 40S60. This pressure vessel housed a membrane module with a 4040 configuration that we had developed in our laboratory. The thin film composite membrane for BWRO that we used in our module was based on polyamide, and our module-winding protocol was described in our earlier work (Sutariya *et al.* 2022a). The average membrane area in our lab-developed SWM module is around 6.1 m^2 (Sutariya *et al.* 2022a). To control the pressure in the system, a needle valve manufactured by Valson Valves India was used in the reject line. Both the reject and product were recirculated back to the feed tank. The piping used in the low-pressure region was made of PVC, whereas the piping used in the high-pressure region was made of wire-braided hydraulic hoses. The described plant was designed for the delivery of 250 L of desalinated water per hour.

Various locations on the plant are marked from 0 to 6 (Figure 1). To measure the pressure at some of those locations, we used pressure gauges of appropriate ranges. These gauges were procured from Micro Process Controls, India. The synthetic feed solution was prepared by adding NaCl (Fisher Scientific, 99.9% pure) into RO-treated water. To measure the conductivity of the feed, permeate, and reject stream, we used the Eutech conductivity meter (PC2700). Based on the conductivity data, the salt rejection performance was assessed under different operating conditions. Since the synthetic feed consisted only of NaCl in RO-treated water, no fouling or scaling was expected on the membrane. The membrane was stabilized for 1 h each at different operating pressures before taking the samples for analysis and measurement. The samples were collected thrice and the mean readings were recorded in each case.

2.2. Mathematical analysis

In the context of the considered case, small variations in water properties that arise from changes in salinity, such as density or specific volume, and the effect of chemical potential on exergy (Mostafa *et al.* 2011) were deemed insignificant and were therefore ignored. To calculate the relative increase in the rate of exergy flow at different locations within the plant, the exergy

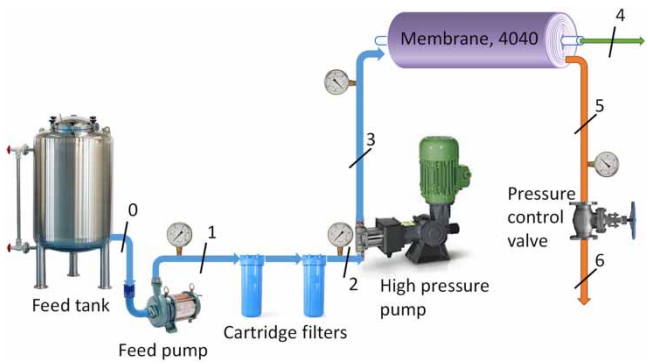

Figure 1 | The schematic representation of the community-scale BWRO plant.

of the feed in each case was used as the reference for that particular case. In each case of feed salinity, the dead state was considered under the same salinity level with a temperature of 30 °C and atmospheric pressure. Various methods available for exergy analysis are discussed by Fellaou *et al.* (2021), e.g. the Cerci model (Cerci 2002), the Drioli model (Francesca & Enrico 2010), and the Sharqawy model (Mostafa *et al.* 2011). We considered the Cerci model for simplicity, as the salt concentration in the feed is not significant in comparison to seawater or hypersaline water.

The mass fraction of the salt, m_s, in a saline solution, is expressed in terms of its salinity value, mg/L as:

$$m_s = \frac{\text{mg/L}}{10^6} \tag{1}$$

The mass fraction of water, m_w, can be calculated from:

$$m_s + m_w = 1 \tag{2}$$

From the mass fraction, the mole fraction of salt, M_s, can be expressed as:

$$M_s = \frac{18}{58.5(1/m_s - 1) + 18} \tag{3}$$

The mole fraction of water, M_w, can be calculated from:

$$M_s + M_w = 1 \tag{4}$$

The properties like enthalpy, h, and entropy, s, of the solution at various marked locations in Figure 1 are required for exergetic calculations, as the exergy, ψ, is defined as:

$$\psi = h - h_0 - T_0(s - s_0) \tag{5}$$

The superscript 0 refers to the dead state. In general, h of the flow stream is defined as:

$$h = m_s h_s + m_w h_w \tag{6}$$

Mixing salt in water is an irreversible process. As a result, the entropy of a mixture at a particular temperature and pressure must be higher than the sum of the entropies of the individual components before mixing at the same temperature and pressure. Hence, the entropy of the saline flow stream is defined for the considered ideal mixture as:

$$s = m_s s_s + m_w s_w - R_m(M_s ln\, M_s + M_w \ln mM_w) \tag{7}$$

where s_s and s_w are the independent entropies of salt and water, respectively at the same temperature and pressure. The water properties can be determined from the water and steam table. Further, R_m is defined as:

$$R_m = \frac{R_u}{N_m} \tag{8}$$

R_u is the universal gas constant and N_m is the molar mass of the saline flow stream, given as:

$$N_m = M_s \times 58.5 + M_w \times 18 \tag{9}$$

Further, the salt properties, $h_{s,}$ and s_s are independent of pressure. Moreover, there is no temperature variation in this study. Hence, these properties remain constant (equal to 25.104 kJ/kg and 0.08722 kJ/kg K, respectively Kahraman & Cengel (2005)) for each marked location in Figure 1.

The rate of flow of exergy can finally be calculated as:

$$\dot{\psi} = \dot{m}[h - h_0 - T_0(s - s_0)] \tag{10}$$

where $\dot{m}$ is the mass flow rate of the stream.

The following equations were considered for analysis of the captured data:

$$\begin{aligned}\text{Rate of exergy addition by the pumps} = {} & \text{Rate of flow of exergy through feed pump} + \\ & \text{Rate of flow of exergy through HP pump}\end{aligned} \tag{11}$$

$$\begin{aligned}\text{The minimum rate of separation work} = {} & \text{Flow of exergy with product water} + \\ & \text{Flow of exergy with reject water} - \\ & \text{Flow of exergy with feed water}\end{aligned} \tag{12}$$

The salinity of the reject stream was adjusted by a mass balance of the feed stream and the product stream in each case to calculate the minimum work of separation accurately:

$$\text{Exergetic efficiency} = \frac{\text{Minimum rate of separation work}}{\text{Rate of exergy addition by the pumps}} \tag{13}$$

The total dissolved solids in the reject water were adjusted as per the mass balance.

3. RESULTS AND DISCUSSION

The thermodynamic analysis of the plant operating at different conditions involved the evaluation of specific exergy and exergy flow rate, which are presented in Table 1 (operating pressure: 13.79 bar or 200 psi), Table 2 (operating pressure: 20.68 bar or 300 psi), and Table 3 (operating pressure: 27.58 bar or 400 psi).

Table 4 provides a more detailed analysis of exergy losses due to inefficiencies of the pumps and pressure drop across various components. This table also presents the fraction of exergy loss for different components, such as the feed pump, cartridge filters, HP pump, membrane, and pressure control valve for operation at 13.79, 20.68, and 27.58 bar. The detailed methodology of the calculations involved is mentioned in the supplementary material. This analysis helped in understanding the causes of exergy loss and in identifying the components that required improvement. It could be observed that the feed flow rate was nearly constant (0.38–0.3883 kg/s) at different pressures because of the positive displacement pump.

The salt rejection and permeate flux of the membrane were critical factors that affected the exergetic efficiency of the plant. The results in Table 4 showed that higher permeate flux (corresponding to higher permeate recovery) and salt rejection led to a higher amount of required separation work at any feed concentration. Correspondingly, the exergetic efficiency of the plant also increased with pressure across the feed salinity range.

The exergetic efficiency of the BWRO plant of this scale with the used components was very low, ranging from 0.01 to 0.51% (Table 4) under varying salinity and operating pressure within the considered range. The components through which the most exergy destruction occurred were the HP pump and the pressure control valve. The effect of various components and operating parameters are described as follows in detail.

3.1. Feed pump

The feed pump assembly was responsible for providing the necessary pressure to force the feed water through the pre-treatment system (cartridge filter in this case). In doing so, it required a significant amount of energy, which contributed to the overall exergy destruction in the system. The efficiency of the feed pump was calculated by taking the ratio of the exergy added by it to the feed stream and the electric power consumed by it. The average efficiencies measured at various operating pressures were consistently low (≈9%). Moreover, the efficiency showed little variation with changes in salinity. Also, it was relatively constant across different operating pressures, indicating that the inefficiencies of the feed pump assembly were not significantly affected by changes in the operating conditions. The reason was that the pressure developed by the feed pump was not significantly affected by the overall operating pressure in the BWRO system.

Table 1 | Analysis of specific exergy and exergy flow rate with various feed solutions at an operating pressure of 13.79 bar

		2,000 mg/L feed				10,000 mg/L feed				20,000 mg/L feed			
Location	Operating pressure (bar)	Salinity (mg/L)	Mass flow rate (kg/s)	Specific exergy (kJ/kg)	Exergy flow rate (KW)	Salinity (mg/L)	Mass flow rate (kg/s)	Specific exergy (kJ/kg)	Exergy flow rate (KW)	Salinity (mg/L)	Mass flow rate (kg/s)	Specific exergy (kJ/kg)	Exergy flow rate (KW)
0	0	2,000	0.3883	0	0	10,000	0.3883	0	0	20,000	0.3883	0	0
1	1	2,000	0.3883	0.0989	0.0384	10,000	0.3883	0.0981	0.0381	20,000	0.3883	0.0971	0.0377
2	0.7	2,000	0.3883	0.0724	0.0281	10,000	0.3883	0.0718	0.0279	20,000	0.3883	0.0711	0.0276
3	14	2,000	0.3883	1.4174	0.5504	10,000	0.3883	1.4060	0.5460	20,000	0.3883	1.3918	0.5405
4	0	43	0.03	0.6899	0.0207	458	0.0142	2.6745	0.0379	6,760	0.0018	3.0940	0.0057
5	13.79	2,164	0.3583	1.3331	0.4777	10,361	0.3742	1.2846	0.4807	20,063	0.3865	1.3458	0.5202
6	0	2,164	0.3583	−0.0511	−0.0183	10,361	0.3742	−0.0882	−0.0330	20,063	0.3865	−0.0136	−0.0053

Table 2 | Analysis of specific exergy and exergy flow rate with various feed solutions at an operating pressure of 20.68 bar

		2,000 mg/L feed				10,000 mg/L feed				20,000 mg/L feed			
Location	Absolute pressure (bar)	Salinity (mg/L)	Mass flow rate (kg/s)	Specific exergy (kJ/kg)	Exergy flow rate (KW)	Salinity (mg/L)	Mass flow rate (kg/s)	Specific exergy (kJ/kg)	Exergy flow rate (KW)	Salinity (mg/L)	Mass flow rate (kg/s)	Specific exergy (kJ/kg)	Exergy flow rate (KW)
0	0	2,000	0.384	0	0	10,000	0.384	0	0	20,000	0.384	0	0
1	1	2,000	0.384	0.0989	0.0380	10,000	0.384	0.0981	0.0377	20,000	0.384	0.0971	0.0373
2	0.7	2,000	0.384	0.0724	0.0278	10,000	0.384	0.0718	0.0276	20,000	0.384	0.0711	0.0273
3	21	2,000	0.384	2.0495	0.7870	10,000	0.384	2.0331	0.7807	20,000	0.384	2.0125	0.7728
4	0	34	0.0467	0.6942	0.0324	296	0.0283	2.7365	0.0775	1,707	0.0098	4.5150	0.0442
5	20.68	2,272	0.3373	1.9960	0.6733	10,775	0.3557	1.8740	0.6665	20,500	0.3742	1.9390	0.7256
6	0	2,272	0.3373	−0.0845	−0.0285	10,775	0.3557	−0.1888	−0.0672	20,500	0.3742	−0.1036	−0.0388

Table 3 | Analysis of specific exergy and exergy flow rate with various feed solutions at an operating pressure of 27.58 bar

		2,000 mg/L feed				10,000 mg/L feed				20,000 mg/L feed			
Location	Absolute pressure (bar)	Salinity (mg/L)	Mass flow rate (kg/s)	Specific exergy (kJ/kg)	Exergy flow rate (KW)	Salinity (mg/L)	Mass flow rate (kg/s)	Specific exergy (kJ/kg)	Exergy flow rate (KW)	Salinity (mg/L)	Mass flow rate (kg/s)	Specific exergy (kJ/kg)	Exergy flow rate (KW)
0	0	2,000	0.38	0	0	10,000	0.38	0	0	20,000	0.38	0	0
1	1	2,000	0.38	0.0989	0.0376	10,000	0.38	0.0981	0.0373	20,000	0.38	0.0971	0.0369
2	0.7	2,000	0.38	0.0724	0.0275	10,000	0.38	0.0718	0.0273	20,000	0.38	0.0711	0.0270
3	27.9	2,000	0.38	2.7951	1.0621	10,000	0.38	2.7727	1.0536	20,000	0.38	2.7447	1.0430
4	0	32	0.0667	0.6952	0.0463	244	0.045	2.7572	0.1241	913	0.025	4.7753	0.1194
5	27.58	2,419	0.3133	2.5753	0.8069	10,378	0.3350	2.3630	0.7916	21,334	0.355	2.3647	0.8395
6	0	2,419	0.3133	−0.1296	−0.0406	10,378	0.3350	−0.3178	−0.1065	21,334	0.355	−0.2889	−0.1026

Table 4 | Performance and exergy analysis of the community-scale BWRO plant at different operating pressures

	Operating pressure (bar)	2,000 mg/L	10,000 mg/L	20,000 mg/L
Observed salt rejection (%)	13.79	97.8	95.4	66.2
	20.68	98.3	97	91.5
	27.58	98.4	97.6	95.4
Permeate recovery (%)	13.79	7.7	3.6	0.5
	20.68	12.2	7.4	2.6
	27.58	17.5	11.8	6.6
Exergy addition through pumps (kW)	13.79	$(0.0384-0)+(0.5504-0.0281)=0.5607$	$(0.0381-0)+(0.5460-0.0279)=0.5562$	$(0.0377-0)+(0.5405-0.0276)=0.5506$
	20.68	$(0.038-0)+(0.7870-0.0271)=0.7972$	$(0.0377-0)+(0.7807-0.0276)=0.7908$	$(0.0373-0)+(0.7728-0.0273)=0.7828$
	27.58	$(0.0376-0)+(1.0621-0.0275)=1.0722$	$(0.0373-0)+(1.0536-0.0273)=1.0636$	$(0.0369-0)+(1.0430-0.0270)=1.0528$
Measured electrical power supplied through feed pump (kW)	13.79	0.414		
	20.68	0.414		
	27.58	0.414		
Measured electrical power supplied through HP pump (kW)	13.79	2.737		
	20.68	2.875		
	27.58	3.013		
Total electric power supplied (kW)	13.79	3.151		
	20.68	3.289		
	27.58	3.427		
Minimum work input for desalination (kW)	13.79	$-0.0183+0.0207-0=0.0024$	$-0.0330+0.0379-0=0.0049$	$-0.0053+0.0057-0=0.0004$
	20.68	$-0.0285+0.0324-0=0.0039$	$-0.0672+0.0775-0=0.0104$	$-0.0388+0.0442-0=0.0055$
	27.58	$-0.0406+0.0463-0=0.0057$	$-0.1065+0.1241-0=0.0176$	$-0.1026+0.1194-0=0.0168$
Total exergy destruction (kW)	13.79	3.1486	3.1461	3.1506
	20.68	3.2851	3.2786	3.2835
	27.58	3.4213	3.4094	3.4102
Exergy destruction by feed pump assembly (%)	13.79	11.93	11.95	11.94
	20.68	11.45	11.48	11.47
	27.58	11.00	11.05	11.06
Exergy destruction by HP pump assembly (%)	13.79	70.34	70.53	70.59
	20.68	64.41	64.72	64.85
	27.58	57.83	58.27	58.56
Exergy destruction through RO membrane (%)	13.79	1.65	0.87	0.47
	20.68	2.47	1.12	0.09
	27.58	6.10	4.05	2.47
Exergy destruction through cartridge filters (%)	13.79	0.33	0.32	0.32
	20.68	0.31	0.31	0.30
	27.58	0.29	0.29	0.29
Exergy destruction through pressure control valve (%)	13.79	15.75	16.33	16.68
	20.68	21.36	22.38	23.28
	27.58	24.77	26.34	27.62
Exergetic efficiency (%)	13.79	0.08	0.15	0.01
	20.68	0.12	0.32	0.17
	27.58	0.17	0.51	0.49
Performance of RO (kWh/m^3)	13.79	29.18	61.64	486.26
	20.68	19.56	32.28	93.23
	27.58	14.27	21.15	38.08

Improving the performance of the feed pump assembly could involve replacing it with a suitable pump-motor assembly having high efficiency at this operating point. This could potentially reduce the energy required by the feed pump assembly, leading to a reduction in the exergy destruction and an improvement in the overall efficiency of the desalination system. Other options are the use of a variable frequency drive, replacement of the motor with an energy-efficient motor, timely maintenance of the assembly, etc.

Overall, the high exergy destruction by the feed pump assembly suggested that there was significant room for improvement in the design, operation, and maintenance of the feed pump assembly, which could lead to significant improvements in the efficiency of the desalination system.

3.2. HP pump

The HP pump was responsible for increasing the water pressure to the level required for the RO process. The measured electrical power supplied through the HP pump increased as the operating pressure increased (2.737, 2.875, and 3.013 kW for 13.79, 20.68, and 27.58 bar, respectively), indicating that more energy was needed to increase the water pressure at higher operating pressures.

The average efficiencies of the HP pump assembly were only 18.94, 26.22, and 34.09% at 13.79, 20.68, and 27.58 bar operating pressures, respectively, with a little variation with salinity. The efficiency increased with an increase in operating pressure; correspondingly, the exergy destruction by the HP pump assembly decreased as the operating pressure increased, indicating that more irreversibilities occurred within the pump at lower pressures. The results showed that the highest amount of exergy destruction was observed when the operating pressure was at 13.79 bar. This could be attributed to the fact that fixed losses in the pump-motor assembly are more significant when the operating pressure was low, and the minimum work of separation was also very low (indicated by low permeate recovery and salt rejection).

The exergy destruction through the HP pump assembly was the highest among all components (Figure 2), indicating that it was the most significant source of irreversibility in the system. This implied that efforts should be made to reduce the exergy destruction within the HP pump assembly to improve the overall efficiency of the system. Improving the performance of the HP pump assembly involves similar steps as described for the feed pump assembly, such as replacing it with a suitable pump-motor assembly having high efficiency at this operating point, use of a variable frequency drive, replacement of the motor with an energy-efficient motor, timely maintenance of the assembly, etc.

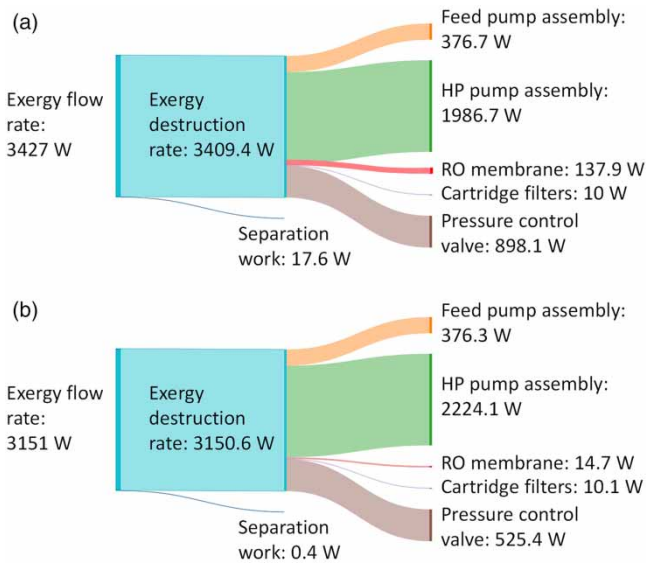

Figure 2 | Exergy flow charts corresponding to (a) highest exergetic efficiency achieved (with 10,000 ppm feed and 400 psi operating pressure) and (b) lowest exergetic efficiency achieved (with 20,000 ppm feed and 200 psi operating pressure). It could be observed that the major contributors to the exergy destruction are the pump assemblies and the pressure control valve.

3.3. Pressure control valve

The pressure control valve was responsible for maintaining the required pressure in the membrane system. From Table 4, it could be observed that the exergy destruction through the pressure control valve increased with increasing operating pressure, with the highest exergy destruction occurring at 27.58 bar for each salinity level. This was because the pressure drop across the pressure control valve increased with the operating pressure.

3.4. Operating pressure

The analysis revealed that at a lower operating pressure of 13.79 bar, the exergetic efficiency was lower, with the HP pump assembly contributing to higher exergy destruction, while the impact of the pressure control valve was comparatively lower. Conversely, the exergetic efficiency improved with pressure, as the exergy destruction caused by the HP pump assembly decreased and that by the pressure control valve slightly increased. Therefore, for the developed system, it is recommended to maintain the highest possible operating pressure (i.e. 27.58 bar here) at all salinity levels to achieve the optimal utilization of exergy.

It was essential to optimize the operating pressure to achieve maximum exergetic efficiency and minimize the exergy destruction by the various components. The optimal operating pressure may vary depending on the specific desalination system and its components. Simultaneously, for practical cases, the fouling propensity of the feed and concentration polarization also plays crucial roles in deciding the optimum operating pressures of the RO systems.

3.5. Feed salinity level

At 2,000 mg/L salinity, the exergy destruction by the HP pump assembly for an operating pressure of 13.79 bar was 70.32%, while for the same operating pressure at 10,000 and 20,000 mg/L salinity, it was 70.5 and 70.57%, respectively. Hence, at a constant operating pressure of 13.79 bar, the exergy destruction by the HP pump assembly varied only slightly as the salinity level increased. The same was the case with the operation at higher pressures. This meant that the salinity level had a negligible effect on the performance of the HP pump assembly. Similarly, the amount of exergy destruction by feed pump assembly was also relatively constant with feed salinity. However, the exergy destruction caused by the pressure control valve was influenced by the feed salinity, particularly at higher operating pressures. At 27.58 bar, for instance, the percentage of exergy destruction varied by approximately 3%.

Based on the experimental data (Table 4), the impact of feed salinity on exergetic efficiency appeared to have an optimum salinity level for maximum efficiency. For instance, at all operating pressures, the highest exergetic efficiency was observed at the feed salinity of 10,000 mg/L.

Although the operating conditions, including feed salinity and operating pressure, had a minimal impact on the exergetic efficiency (with a variation of up to 0.5%), it was primarily due to the low efficiency of the plant components, such as feed pump assembly, HP pump assembly, and pressure control valve. If the efficiency of these components is improved, the impact of the operating parameters on the exergetic efficiency will become more noticeable. For example, if the efficiencies of the pump assemblies are improved to 75% (similar to large-scale systems Kahraman & Cengel (2005)), the variation in the exergetic efficiency was calculated to be more than 1.18%, which was also not significant as the major exergetic losses in this case (60–70%) occurred across the pressure control valve.

The performance of the RO plant, measured in kWh/m^3, exhibited a correlation with the exergetic efficiency of the plant across various operational scenarios. Irrespective of the feed salinity, the performance of the RO system demonstrated improvement with increasing exergetic efficiency (Figure 3). Specifically, the highest level of exergetic efficiency was attained at the maximum operating pressure of 27.58 bar. Moreover, the rate of change of the kWh/m^3 value with respect to exergetic efficiency was found to be higher at lower exergetic efficiency levels, which correspond to higher feed salinity. As we progressed towards higher exergetic efficiency levels, the rate of change became comparatively lower. Furthermore, when comparing different salinity levels at the same operating pressures, higher values of kWh/m^3 for permeate water were achieved with elevated salinity inputs. This outcome was due to the fact that higher salinity feeds yielded a lower quantity of product, as opposed to lower salinity feeds operating under the same pressure conditions.

The feed salinity level is influenced by site conditions, but we have control over the operating pressure. By regulating the pressure, we can achieve maximum exergy utilization while ensuring that the flux through the membrane does not exceed the critical level to prevent membrane fouling (Sutariya *et al.* 2022b) while increasing the pressure. This study revealed that the HP pump assembly caused the most exergy destruction, ranging from 57.78 to 70.65% under different operating conditions.

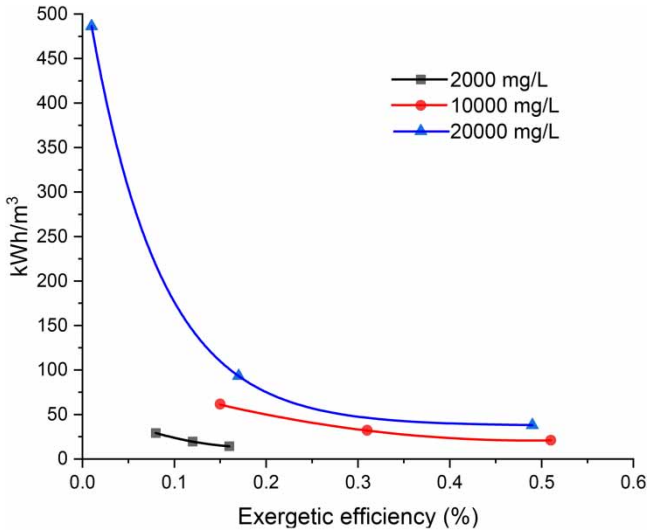

Figure 3 | Performance of the RO plant in terms of kWh/m^3 correlated to the exergetic efficiency at different operating conditions.

This indicated that there was significant scope for enhancing its performance. Various available options to achieve this are upgrading the pump assemblies to energy-efficient assemblies, conducting regular maintenance on pumps, cartridge filters, membranes, etc., or direct coupling of the pump and motor by incorporating a variable frequency drive instead of the belt drive transmission. Implementing these measures can improve the efficiency of the assembly and enhance overall performance.

The study showed that as the pressure in the system increased from 13.79 to 27.58 bar, the exergy destruction across the pressure control valve increased by 9–11% of the total for different salinity levels. This increase in inefficiency would be more noticeable if the performance of the pumps were improved. For instance, if both the pump assemblies had a hypothetical combined efficiency of 75%, the losses across the pressure control valve would range from 60.04 to 70.94%. Since there are no energy recovery devices currently available for these systems, design modifications have been studied to utilize this hydraulic pressure, which has shown promising outcomes (Sutariya & Raval 2021, 2022). In the same manner, future research should focus on saving the hydraulic energy of the reject stream, which would improve the efficiency of BWRO systems. Regular maintenance of the cartridge filters is also recommended to reduce pressure drop across them. These measures can contribute to enhancing the overall performance and sustainability of community-scale BWRO systems.

4. CONCLUSION

Based on the results presented in the study, it was concluded that the performance of the desalination plant was highly dependent on the efficiency of individual components and also slightly on the operating conditions. The detailed analysis of exergy losses due to inefficiencies of pumps and pressure drop across various components helped in identifying the components that required improvement. The HP pump assembly and pressure control valve were found to be major contributors to exergy losses. Similarly, the efficiency of the feed pump assembly was also causing significant destruction of exergy. Improvements in these components can lead to higher exergy efficiency and overall performance of the plant. The analysis further revealed that the exergetic efficiency of the plant was maximum (0.51%) at the feed salinity of 10,000 mg/L and an optimum operating pressure of 27.58 bar. It was minimum (0.01%) for the salinity of 20,000 mg/L and operating pressure of 13.79 bar, due to the low requirement of work of separation and higher fixed losses. Overall, the study provides valuable insights into the thermodynamic behavior of the community-scale membrane-based desalination plant and can serve as a useful guide for future design and optimization of similar systems.

ACKNOWLEDGEMENTS

A PRIS number CSIR-CSMCRI-44/2023 has been allotted to this manuscript. The author acknowledges the financial support from the Council of Scientific and Industrial Research (CSIR), Ministry of Science and Technology, Government of India, to carry out this work.

DATA AVAILABILITY STATEMENT

All relevant data are included in the paper or its Supplementary Information.

CONFLICT OF INTEREST

The authors declare there is no conflict.

REFERENCES

Ahmed, A. A.-G. 2017 Recycling of reverse osmosis (RO) reject streams in brackish water desalination plants using fixed bed column softener. *Energy Procedia* **107**, 205–211. https://doi.org/10.1016/j.egypro.2016.12.174.

Ahmed, Q. B. & Syed, M. Z. 2016 Exergetic efficiency of NF, RO and EDR desalination plants. *Desalination* **378**, 92–99. https://doi.org/10.1016/j.desal.2015.09.027.

Aljundi, I. H. 2009 Second-law analysis of a reverse osmosis plant in Jordan. *Desalination* **239** (1–3), 207–215.

Alsarayreh, A. A., Al-Obaidi, M. A., Ruiz-García, A., Patel, R. & Mujtaba, I. M. 2022 Thermodynamic limitations and exergy analysis of brackish water reverse osmosis desalination process. *Membranes* **12** (1), 11.

Anas, S., Benedikt, B., Mathias, E. & Martin, K. 2021 Decentralized brackish water reverse osmosis desalination plant based on PV and pumped storage – Technical analysis. *Desalination* **516**, 115232. https://doi.org/10.1016/j.desal.2021.115232.

Boretti, A. & Rosa, L. 2019 Reassessing the projections of the world water development report. *NPJ Clean Water* **2** (1), 15. https://doi.org/10.1038/s41545-019-0039-9.

Bouzayani, N., Galanis, N. & Orfi, J. 2009 Thermodynamic analysis of combined electric power generation and water desalination plants. *Applied Thermal Engineering* **29** (4), 624–633. https://doi.org/10.1016/j.applthermaleng.2008.03.031.

Cerci, Y. 2002 Exergy analysis of a reverse osmosis desalination plant in California. *Desalination* **142** (3), 257–266.

Eshoul, N. M., Agnew, B., Al-Weshahi, M. A. & Atab, M. S. 2015 Exergy analysis of a two-pass reverse osmosis (RO) desalination unit with and without an energy recovery turbine (ERT) and pressure exchanger (PX). *Energies* **8** (7), 6910–6925.

Eshoul, N., Agnew, B., Al-Weshahi, M. & Latrash, F. 2016 Exergy analysis of two-pass reverse osmosis (RO) desalination with and without energy recovery turbine (ERT). *International Journal of Exergy* **19** (1), 1–14.

Eshoul, N. M., Agnew, B., Anderson, A. & Atab, M. S. 2017 Exergetic and economic analysis of two-pass RO desalination proposed plant for domestic water and irrigation. *Energy* **122**, 319–328.

Fellaou, S., Ruiz-Garcia, A. & Gourich, B. 2021 Enhanced exergy analysis of a full-scale brackish water reverse osmosis desalination plant. *Desalination* **506**, 114999. https://doi.org/10.1016/j.desal.2021.114999.

Francesca, M. & Enrico, D. 2010 An exergetic analysis of a membrane desalination system. *Desalination* **261** (3), 293–299. https://doi.org/10.1016/j.desal.2010.06.070.

Im, S. J., Jeong, S. & Jang, A. 2021 Forward osmosis (FO)-reverse osmosis (RO) hybrid process incorporated with hollow fiber FO. *npj Clean Water* **4** (1), 51. https://doi.org/10.1038/s41545-021-00143-0.

Joshi, S., Ghosh, P., Shah, V., Devmurari, C., Trivedi, J. & Rao, P. 2004 CSMCRI experience with reverse osmosis membranes and desalination: Case studies. *Desalination* **165**, 201–208.

Kahraman, N. & Cengel, Y. A. 2005 Exergy analysis of a MSF distillation plant. *Energy Conversion and Management* **46** (15), 2625–2636. https://doi.org/10.1016/j.enconman.2004.11.009.

Kahraman, N., Cengel, Y. A., Wood, B. & Cerci, Y. 2005 Exergy analysis of a combined RO, NF, and EDR desalination plant. *Desalination* **171** (3), 217–232. https://doi.org/10.1016/j.desal.2004.05.006.

Mostafa, H. S., Syed, M. Z. & John, H. L. 2011 Second law analysis of reverse osmosis desalination plants: An alternative design using pressure retarded osmosis. *Energy* **36** (11), 6617–6626. https://doi.org/10.1016/j.energy.2011.08.056.

Mushtaque, A., Aro, A., David, H., Muralee, R. T., Mattheus, F. A. G., Mansour, A.-H. & Abdullah, A.-B. 2003 Feasibility of salt production from inland RO desalination plant reject brine: A case study. *Desalination* **158** (1), 109–117. https://doi.org/10.1016/S0011-9164(03)00441-7.

Nuri, M. E., Brian, A., Alexander, A. & Mohanad, S. A. 2017 Exergetic and economic analysis of two-pass RO desalination proposed plant for domestic water and irrigation. *Energy* **122**, 319–328. https://doi.org/10.1016/j.energy.2017.01.095.

Que, V. N. X., Van Tuan, D., Huy, N. N. & Le Phu, V. 2021 Design and performance of small-scale reverse osmosis desalination for brackish water powered by photovoltaic units: a review. In: International Conference on Environment, Resources and Earth Sciences 1–5 December 2020, Ho Chi Minh City, Vietnam.

Romero-Ternero, V., Garcia-Rodriguez, L. & Gómez-Camacho, C. 2005 Exergy analysis of a seawater reverse osmosis plant. *Desalination* **175** (2), 197–207.

Sutariya, B. & Raval, H. 2021 Analytical study of optimum operating conditions in a semi-batch closed-circuit reverse osmosis (CCRO) process. *Separation and Purification Technology* **264**, 118421. DOI: https://doi.org/10.1016/j.seppur.2021.118421.

Sutariya, B. & Raval, H. 2022 Energy and resource-efficient reverse osmosis system with tunable recovery for brackish water desalination and heavy metal removal. *Water and Environment Journal* **36** (4), 579–589. https://doi.org/10.1111/wej.12788.

Sutariya, B., Patel, K. & Karan, S. 2022a Effects of manual interventions in the winding process on the performance of spiral wound membrane module. *Desalination and Water Treatment* **251**, 1–6. https://doi.org/10.5004/dwt.2022.27858.

Sutariya, B., Sargaonkar, A. & Raval, H. 2022b Methods of visualizing hydrodynamics and fouling in membrane filtration systems: Recent trends. *Separation Science and Technology* **57**, 1–30. https://doi.org/10.1080/01496395.2022.2089585.

Tra, N. M. T., Quoc, D. B., Hideaki, S., Yasuhisa, N., Sandrine, B., Hitoshi, K., Haruka, T., Wibawa, S. S. C. & Takahiro, F. 2022 Membrane distillation for achieving high water recovery for potable water reuse. *Chemosphere* **288**, 132610. https://doi.org/10.1016/j.chemosphere.2021.132610.

First received 8 May 2023; accepted in revised form 1 September 2023. Available online 13 September 2023